

# Chaotic hypothesis and anomalous diffusion in coupled symplectic maps

Eduardo G. Altmann and Holger Kantz  
*Max Planck Institute for the Physics of Complex Systems,  
 Nöthnitzer Strasse 38, 01187 Dresden, Germany.*  
 (Dated: February 9, 2020)

We investigate the high dimensional Hamiltonian chaotic dynamics in  $N$  coupled area-preserving maps. We show the existence of an enhanced trapping regime caused by trajectories performing a random walk *inside* the area corresponding to regular islands of the uncoupled maps. As a consequence, we observe long intermediate regimes of power-law decay of the recurrence time statistics (with exponent  $\gamma = 0.5$ ) and of ballistic motion. The asymptotic decay of correlations and anomalous diffusion depend on the stickiness of the  $N$ -dimensional invariant tori. Detailed numerical simulations show weaker stickiness for increasing  $N$  suggesting that high-dimensional Hamiltonian systems asymptotically fulfill the demands of the usual chaotic hypotheses.

## I. INTRODUCTION

Chaotic hypotheses are keystone requisites for both basic theories (statistical mechanics [1, 2]) and computation methods (transport properties [2], elimination of chaotic variables [3]). The different chaotic hypotheses consist essentially of two main assumptions about the (high-dimensional Hamiltonian) dynamics: (i) ergodicity, i.e., the existence of a single chaotic component and negligible measure of the regions of quasi-periodic motion; and (ii) strong mixing (exponential decay of correlations). Generic low-dimensional Hamiltonian systems violate both hypotheses since the chaotic trajectories stick to the border of islands of regular motion introducing long-term correlations in the dynamics [4, 5, 6].

For many higher dimensional systems it is generally expected that hypothesis (i) is effectively valid since the measure of the quasi-periodic trajectories typically decreases (exponentially) with the number  $N$  of degrees of freedom (see, e.g., Sec. 6.5 of Ref. [7]). However, the vanishing measure of regular regions [hypothesis (i)] does not guarantee the fast decay of correlations [hypothesis (ii)]. The breakdown of hypothesis (ii) occurs due to the trapping (stickiness) of chaotic trajectories around non-hyperbolic structures in the phase-space, and even zero measure sets (e.g., the bouncing ball orbits in the Bunimovich stadium billiard) can be responsible for the anomalous decay of correlations [8, 9]. Considerable progress has been achieved for the problem of trapping in area-preserving maps ( $N = 1$ ) [4, 5, 6], while only few numerical results are known for  $N = 2-5$  [10, 11]. On the other hand, higher dimensional systems are usually considered for the calculation of different properties, such as relaxation phenomena [12] and diffusion [13, 15].

In this Paper we perform a detailed study of the trapping properties of Hamiltonian systems with an increasing number of degrees of freedom by coupling  $N$  area-preserving maps [10, 13]. This system typically has invariant tori, but hypothesis (i) is satisfied for large  $N$  in the sense mentioned above (our results do not apply when regular behavior prevails for  $N \rightarrow \infty$  [14]). For weak coupling we observe an intermediate regime of enhanced trapping which we show to exist also for area-

preserving maps perturbed by noise. Asymptotically, our numerical results show that the trapping decreases with  $N$  indicating the effective validity of hypothesis (ii) for high-dimensional Hamiltonian systems composed of coupled low-dimensional ones, provided ergodicity is approached. Additionally, we show how the different trapping regimes impact on the anomalous diffusion of the perturbed standard map and lead to a non-trivial dependence of the asymptotic diffusion coefficient on the perturbation strength, clarifying previous conflicting results [13, 15, 16, 17].

## II. COUPLED SYMPLECTIC MAPS

We construct a time-discrete  $2N$ -dimensional Hamiltonian system by the composition  $\mathbf{T} \circ \mathbf{M}$  of the independent one-step iteration of  $N$  symplectic 2-dimensional maps  $\mathbf{M} = (M_1, \dots, M_N)$  and a symplectic coupling  $\mathbf{T} = (T_1, \dots, T_N)$ . As a representative example of 2-d maps we choose for our numerical investigation the standard map [7]:

$$M_i \begin{pmatrix} p_i \\ q_i \end{pmatrix} = \begin{pmatrix} p_i + K_i \sin(2\pi q_i) \pmod{1} \\ q_i + p_i + K_i \sin(2\pi q_i) \pmod{1} \end{pmatrix}, \quad (1)$$

and a coupling potential between the maps  $i, j$  given by  $V_{i,j} = \xi_{i,j} \cos[2\pi(q_j - q_i)]$  [22]. The action of the coupling on the  $i$ -th map is hence given by

$$T_i \begin{pmatrix} p_i \\ q_i \end{pmatrix} = \begin{pmatrix} p_i + \sum_{j=1}^N \xi_{i,j} \sin[2\pi(q_i - q_j)] \\ q_i \end{pmatrix}, \quad (2)$$

what corresponds to a perturbation  $\Delta p_i$ . The full coupling  $\mathbf{T}$  is symplectic provided  $\xi_{i,j} = \xi_{j,i}$ . For simplicity we use all-to-all coupling with  $\xi_{i,j} = \frac{\xi}{\sqrt{N-1}}$ , in which case a numerically convenient mean-field representation can be written [12]

$$\Delta p_i = \frac{\xi}{\sqrt{N-1}} \sum_{j=1}^N \sin[2\pi(q_i - q_j)] = \xi |\mathbf{m}| \sin(2\pi q_i - \phi), \quad (3)$$

where  $\mathbf{m} = (m_x, m_y) = \frac{1}{\sqrt{N-1}} \sum_j [\cos(q_j), \sin(q_j)]$  and  $\tan(\phi) = m_y/m_x$ . When the isolated systems are chaotic and weakly coupled we can assume that the positions  $q_j$  are uncorrelated and approximate each term of the sum in Eq. (3) by a random variable  $y \in ]-1, 1[$  distributed according to the density  $P(y) = 1/(2\pi\sqrt{1-y^2})$ , which has variance  $\sigma_y = \sqrt{2}/2$ . Additionally, for large  $N$  Eq. (3) tends to a normal distribution with  $\sigma = \xi\sigma_y$ , i.e., a finite perturbation strength. This is a major difference from other coupled-map models (where a rescale term  $1/N$  instead of  $1/\sqrt{N-1}$  is used)[12, 14].

### III. TRAPPING IN THE MODEL

#### A. Standard map perturbed by noise

Motivated by the previous considerations we study initially the trapping properties of one standard map perturbed by white noise, i.e, we replace Eq. (3) by  $\Delta p_1 = \xi\delta$ , where  $\delta$  is a Gaussian distributed random number with zero mean and variance  $\sigma = \sigma_y$ . We fix  $K_1 = 0.52$  in (1), where a single large regular island is visible in the phase space (inset of Fig. 1), what facilitates the interpretation of our results. The trapping is measured by regimes of power-law decay of the recurrence time statistics (RTS)  $\rho(\tau) \sim \tau^{-\gamma}$ , defined as the probability of a trajectory to return at a time  $T > \tau$  to a pre-defined region. During the long recurrence times the trajectory performs almost a quasi-periodic motion leading to a power-law decay of correlations with exponent  $\gamma_c = \gamma - 1$  [4]. We have iterated a single trajectory  $10^{12}$  times and recorded the times  $T$  between successive recurrences to a large region away from the island. The RTS for different noise intensities  $\xi$  is shown in Fig. 1. Three different noise regimes can be identified for small  $\xi$ :

**(R1)** For short times ( $\tau < \tau_{1,2}$ ) the RTS follows the unperturbed one ( $\xi = 0$ ), i.e., it shows an exponential followed by a power-law decay (with exponent  $\gamma_{R1}$ ).

**(R2)** For intermediate times ( $\tau_{1,2} < \tau < \tau_{2,3}$ ) the RTS shows an enhanced trapping due to trajectories that entered the island through the action of the noise. Once inside the island the trajectories circle the central elliptic periodic orbit and perform a random walk in the perpendicular direction. The power-law exponent tends to the value of a random walker  $\gamma_{R2} \approx \gamma_{RW} = 0.5$ . As in typical RTS of Hamiltonian systems, we observe additionally log-periodic oscillations.

**(R3)** For long times ( $\tau > \tau_{2,3}$ ) the RTS decays exponentially.

We obtain now the dependence of  $\tau_{1,2}$  and  $\tau_{2,3}$  on  $\xi$ . The starting time of (R2),  $\tau_{1,2}$ , occurs when the displacement due to the noise is of the same size of the chaotic layer between two cantori where the trajectory is stuck. Using the Markov-tree model for stickiness introduced in Ref. [5], the authors of Ref. [16] obtained

$$\tau_{1,2} \sim \xi^{-\beta}, \quad (4)$$

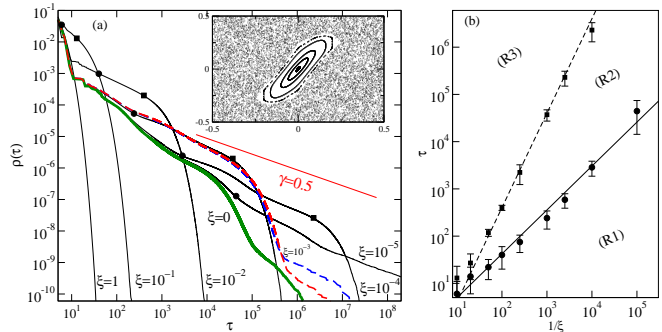


FIG. 1: (Color online) (a) RTS for the standard map with  $K = 0.52$ . The thick solid line corresponds to the unperturbed case ( $\xi = 0$ ), whose phase space is shown in the inset. The thin solid lines correspond to perturbations due to white noise with  $\xi = 10^0, \dots, 10^{-5}$  (from left to right). In each curve  $\tau_{1,2}$  ( $\bullet$ ) and  $\tau_{2,3}$  ( $\blacksquare$ ) are indicated. The dashed lines correspond to the cases of two (upper) and three (lower) coupled standard-maps with  $\xi = 10^{-3}$  and  $K_i \approx 0.52$ . (b) Dependence of  $\tau_{1,2}$  and  $\tau_{2,3}$  on  $\xi$ :  $\tau_{1,2} = 0.58\xi^{-0.93}$  (upper line) in agreement with Eq. (4); and  $\tau_{2,3} = 0.04\xi^{-2}$  (lower line) in agreement with Eq. (5).

with  $\beta = 1/(2\gamma_{R1} - 1)$ . Since usually  $1 < \gamma_{R1} < 2$  we obtain  $1/3 < \beta < 1$ . Differently from Ref. [16], we observe the onset of the exponential regime (R3) at the time  $\tau_{2,3} > \tau_{1,2}$ , due to the finiteness of the random walk domain. Considering the measure  $\mu_I$  of the (largest) island inside which a random walker (with step size proportional to  $\xi$ ) performs a diffusive motion, the dependence of  $\tau_{2,3}$  on  $\xi$  can be estimated as

$$\tau_{2,3} \sim \mu_I \xi^{-2}. \quad (5)$$

In Fig. 1b we verify the agreement of Eqs. (4) and (5) with the values estimated numerically. The numerical values of  $\tau_{1,2}$  and  $\tau_{2,3}$  were estimated as the intersecting point of two fitted power-laws (or exponential), which extend over more than two decades for small  $\xi$  and can be extrapolated for higher  $\xi$ . The noise has two qualitatively different effects: while (R3) represents the typical cutoff of the power-law distribution [16], during the novel regime (R2) the noise acts constructively (increasing the regularity of the dynamics) by allowing trajectories to penetrate the regular island.

#### B. Higher dimensional Hamiltonian system

We investigate now the fully deterministic system given by the composition of Eqs. (1) and (2). The existence of  $N$ -dimensional invariant tori is confirmed for small coupling by the application of the Kolmogorov-Arnold-Moser theorem to the tori build as a direct product of the 1-dimensional tori of the  $N$  uncoupled maps (the quasi-periodic orbits inside the island). All our numerical simulations for  $\xi \leq 0.1$  are consistent with the assumption that these are the only existent tori, in

agreement with a more general picture of Hamiltonian systems: exponential decay of the measure of the tori with  $N$  ( $\mu_{\text{tori}} = \mu_I^N$  for  $\xi \rightarrow 0$ ) and nonexistence of tori of dimension smaller than  $N$  – “Froeschlé conjecture” [7]. Furthermore, due to Arnold diffusion, a single chaotic ergodic component exists. This means that the motion in the  $2N$ -dimensional phase space belongs to *the* chaotic component if the variables of at least one map belong to its chaotic component when uncoupled.

The numerical RTS obtained for  $N > 1$  and for the noisy model are almost indistinguishable for recurrence times belonging to the regimes (R1) and (R2). Two representative examples – for  $\xi = 10^{-3}$  and  $N = 2, 3$  – are depicted as dashed lines in Fig. 1[23]. Remarkable differences are observed in regime (R3), which are analyzed in detail in Fig.2a for  $\xi = 0.05$ , and show that:

**(R3’)** For large times ( $\tau > \tau_{2,3}$ ) the RTS shows an exponential followed by a power-law decay (with exponent  $\gamma_{R3}$ ) due to the stickiness to  $N$ -dimensional tori [10].

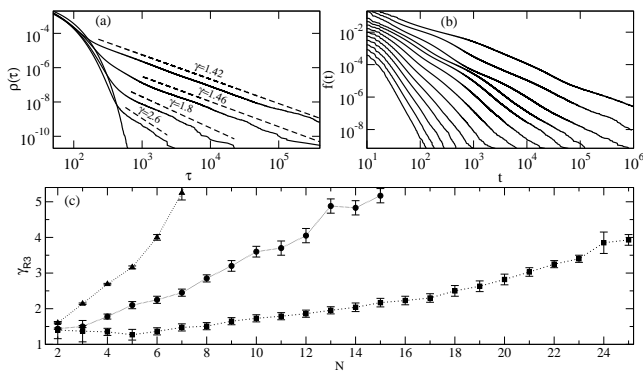


FIG. 2: (a) RTS for  $\xi = 0.05$  and  $N = 2, 3, 4, 5$ , and noise (from top to bottom). (b) Survival probability  $f(t)$  of  $10^{10}$  trajectories near the  $N$ -dimensional tori for  $\xi = 0.05$  and  $N = 2, \dots, 15$  (from top to bottom). (c) Exponent  $\gamma_{R3}$  fitted to the power-law regime of  $f(t)$  for  $\xi = 0.1, 0.05, 0.03$  (from top to bottom). In all cases  $K_1 = 0.52$  and  $K_i \in [0.51, 0.53]$ ,  $i \in \{2, \dots, N\}$  were used in map (1).

We investigate next the dependence on  $N$  of the asymptotic power-law exponent  $\gamma_{R3}$ , what corresponds to a pure high-dimensional effect. The term asymptotic here has to be taken with caution since already for  $N = 1$  the convergence is very slow [4]. However, for our purposes it is enough to perform a comparative analysis for different  $N$  and similar times and initial conditions. It is necessary to distinguish between two effects of  $N$  on the RTS seen in Fig. 2a: the later onset of the power-law regime for increasing  $N$ , related to the smaller measure of the tori – hypothesis (i); and the different values of  $\gamma_{R3}$  (slopes of the tails), related to the stickiness to higher dimensional tori – hypothesis (ii) investigated here. Figure 2a already suggests that  $\gamma_{R3}$  increases with  $N$ . In Ref. [10] similar results were reported for a different system and  $N = 2$  and 3. For improved statistics in the tails we study the survival probability  $f(t)$  inside a re-

gion containing the  $N$ -dimensional tori of  $10^{10}$  trajectories started *close* to them [24].  $f(t)$  is shown in Fig. 2b where it is evident that the power-law exponent increases with  $N$ . The estimated exponents shown in Fig. 2c for different moderate values of the coupling  $\xi$  suggest a linear dependence  $\gamma_{R3} \propto N$ . This result is consistent with hypothesis (ii) for high-dimensional systems since the sharp tails indicate fast decay of correlations.

#### IV. ANOMALOUS DIFFUSION

One of the most important effects induced by the stickiness is the anomalous diffusion of chaotic trajectories. We consider next the influence of the trapping regimes (R1-3) discussed above on the widely studied case of diffusion in the momentum  $p$  of the standard map [6, 7, 18]. The diffusion is measured considering the map (1) opened in  $p$  and calculating the temporal evolution of the dispersion of an ensemble of trajectories:  $\langle \Delta p^2(t) \rangle = Dt^\nu$ . Diffusion is normal if  $\nu = 1$ . It is well-known that anomalous superdiffusion  $1 < \nu < 2$  is obtained for the parameters  $K$  of the standard map where the so-called accelerator modes (ballistic islands of the open map) exist [6, 7, 18]. The diffusion exponent  $\nu$  is directly linked to the exponent  $\gamma$ , of the trapping of chaotic trajectories around accelerator modes, by [18]

$$\nu = \begin{cases} 2 & \text{if } \gamma < 1, \\ 3 - \gamma & \text{if } 1 \leq \gamma \leq 2, \\ 1 & \text{if } \gamma > 2. \end{cases} \quad (6)$$

Previous publications report numerical results that emphasize different effects of the noise on the diffusion: while in Refs. [15, 16] the onset of normal diffusion was obtained, in Ref. [17] the possible enhancement of anomalous diffusion was reported. Applying the results described above we show that actually both effects exist for different time scales.

The three trapping regimes (R1-3) induce different diffusion regimes, as shown in Fig. 3 and described below. During (R1) the anomalous diffusion is similar to the unperturbed case. In (R2) the trapping exponent tends to  $\gamma_{R2} = 0.5$  and ballistic motion  $\nu = 2$  is predicted according to Eq. (6). We have verified numerically that the beginning and end of this regime occur at times proportional to, but greater than, those of (R2) (we denote these times as  $\tau_{1,2}^\dagger$  and  $\tau_{2,3}^\dagger$ , respectively). Asymptotically the exponential RTS in (R3) implies normal diffusion. The asymptotic diffusion coefficient  $D_A = \lim_{t \rightarrow \infty} \langle \Delta p^2(t) \rangle / t$  is determined by the intermediate anomalous regimes and shows a nontrivial dependence on the noise intensity  $\xi$ : for weak noise, Eqs. (4) and (5) indicate that the dominant contribution comes from the ballistic regime associated to (R2) and thus  $D_A \approx [D_{R2}(\tau_{2,3}^\dagger - \tau_{1,2}^\dagger)] \sim \xi^{-2}$ . For stronger noise the major contribution is given by a regime of superdiffusion corresponding approximately to (R1), that can be estimated as  $D_A \approx (D_{R1}\tau_{1,2}^\dagger)^{\nu-1} \sim$

$\xi^{-\beta(1-\nu)} \sim \xi^{(\nu-1)/(5-2\nu)}$ , where  $\nu$  is the unperturbed anomalous diffusion exponent (for small times) which is related to  $\beta$  and  $\gamma$  through Eqs. (4) and (6). Considering the composition of this two effects and joining the multiplicative terms in two fitting parameters  $a, b$  we obtain

$$D_A(\xi) = a \xi^{(\nu-1)/(5-2\nu)} + b \xi^{-2}. \quad (7)$$

In the inset of Fig. 3 we show the remarkable agreement of the numerically obtained diffusion coefficient and expression (7). The exponent  $\nu = 1.45$  was obtained independently by fitting the anomalous diffusion of the unperturbed standard map for small times. Specially interesting is the transition for small  $\xi$  to an asymptotic  $\xi^{-2}$  dependence of  $D_A$ , which is a direct consequence of the nontrivial trapping regime (R2), is absent in the case of 1-d maps (e.g., Pomeau-Manneville maps) [16, 19], and was not previously reported in Refs. [15, 16, 17]. The asymptotic  $\xi^{-2}$  scale was predicted through different arguments in Ref. [20], and can be traced back to the works of Taylor [21].

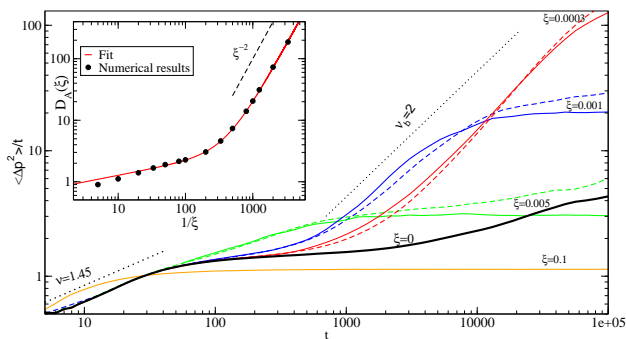


FIG. 3: (Color online) Diffusion in a standard map with  $K_1 = 1.07$  (accelerator mode) coupled to noise (thin solid lines) and to one other standard map with  $K_2 = 0.52$  (dashed lines). The uncoupled case is depicted as a thick solid line. From top to bottom  $\xi = 0.0003, 0.001, 0.005, 0.1$ .  $10^6$  trajectories were used with initial conditions away from islands. When the curves become constant (for  $t \rightarrow \infty$ ) diffusion is normal. Inset: asymptotic diffusion coefficient for different noise intensities. The solid line corresponds to Eq. (7) with  $a = 0.776, b = 1.7 \cdot 10^{-5}$  and  $\nu = 1.45$ .

The diffusion theory described above is valid for noise perturbation and for deterministic high-dimensional sys-

tems whenever  $\gamma_{R3} > 2$  [see Eq. (6)]. When  $\gamma_{R3} < 2$  one observes additionally an asymptotic regime of anomalous diffusion, as shown in Fig. (3) for  $N = 2$  coupled standard maps and different coupling strengths  $\xi$ . We see that the question of whether the asymptotic diffusion is anomalous or normal depends crucially on how the chaotic trajectories stick to  $N$ -dimensional tori (exponent  $\gamma_{R3}$ ). Our results indicate that in general  $\gamma_{R3}$  increases with  $N$  (Fig. 2) and the diffusion is normal, in agreement with Refs. [13, 15]. However, our explanation for this behavior is *not* the absence of hierarchical tori or the Arnold diffusion, as argued in Ref. [13] for a similar system, but simply that  $\gamma_{R3} > 2$  for sufficiently large  $N$ .

## V. CONCLUSION

We have shown that correlations decay faster as the dimensionality  $N$  of a paradigmatic class of Hamiltonian systems increases. More precisely, our numerical simulations show that the asymptotic power-law exponent of the RTS increases with  $N$ , providing evidence that, for large enough  $N$  and times, coupled symplectic maps can be considered for all practical purposes as ergodic and strongly chaotic, satisfying thus the usual chaotic hypotheses. The unexpected observation however is that for small coupling strength or noise intensity a long intermediate enhanced-trapping regime with  $\gamma_{R2} \approx 0.5$  exists due to the trapping inside remnants of lower-dimensional regular regions. This implies a regime of enhanced anomalous diffusion and a non-trivial dependence of the asymptotic diffusion coefficient on the perturbation strength, given by Eq. (7). Applications of these results include noise-perturbed low-dimensional system as well as fully deterministic examples such as galaxy dynamics [11] and active transport [15]. Further investigations are needed to determine whether our results provide a valid description also of systems like Hamiltonian mean field models, where similar transient regimes were observed [12].

## Acknowledgments

E.G.A. thanks G.Cristadoro and A.E.Motter for helpful discussions and CAPES (Brazil) for financial support.

[1] G. Gallavotti and E. G. D. Cohen Phys. Rev. Lett. **74**, 2694 (1995). F. Bonetto et al., J. Stat. Phys. **123**, 39 (2006).  
[2] J.R. Dorfman, *An introduction to chaos in nonequilibrium statistical mechanics* (Cambridge Univ. Press, Cambridge, 1999).  
[3] A. Riebert et al., Phys. Rev. Lett. **94**, 054103 (2005).

[4] B. V. Chirikov and D. L. Shepelyansky, Phys. Rev. Lett. **82**, 528 (1999). M. Weiss, L. Hufnagel, and R. Ketzmerick, Phys. Rev. E **67**, 046209 (2002).  
[5] J. D. Meiss and E. Ott, Phys. Rev. Lett. **55**, 2741 (1985).  
[6] G. M. Zaslavsky, Physics Reports **371**, 461 (2002).  
[7] A. L. Lichtenberg and M. A. Leiberman, *Regular and Chaotic Motion* (Springer-Verlag, New York, 1983).

- [8] E. G. Altmann, A. E. Motter, and H. Kantz, *Phys. Rev. E* **73**, 026207 (2006).
- [9] D. N. Armstead, B. R. Hunt, and E. Ott, *Physica D* **193**, 96 (2004).
- [10] M. Ding, T. Bountis, and E. Ott, *Phys. Lett. A* **151**, 395 (1990). H. Kantz and P. Grassberger, *Phys. Lett. A* **123**, 437 (1987).
- [11] H. E. Kandrup, I. V. Pogorelov, and I. V. Sideris, *Mon. Not. R. Astron. Soc.* **311**, 719 (2000).
- [12] V. Latora, A. Rapisarda, and S. Ruffo, *Phys. Rev. Lett.* **83**, 2104 (1999). M. A. Montemurro, F. Tamarit, and C. Anteneodo, *Phys. Rev. E* **67**, 031106 (2003). M. Antoni, and A. Torcini, *Phys. Rev. E* **57**, R6233 (1998).
- [13] K. Kaneko and T. Konishi, *Phys. Rev. A* **40**, 6130 (1989).
- [14] J.L. Tennyson, J.D. Meiss, and P.J. Morrison, *Physica D* **71**, 496 (1994). D. del-Castillo-Negrete and M.-C. Firpo, *Chaos* **12**, 496 (2005).
- [15] G. Boffetta et al., *Phys. Rev. E* **67** 026224 (2003).
- [16] E. Floriani, R. Mannella, and P. Grigolini, *Phys. Rev. E* **52**, 5910 (1995).
- [17] R. Ishizaki, H. Shibata, and H. Mori, *Prog. Theor. Phys.* **103**, 245 (2000).
- [18] G. Zumofen and J. Klafter, *Europhys. Lett.* **25**, 565 (1994).
- [19] R. Bettin, R. Mannella, B. J. West, and P. Grigolini, *Phys. Rev. E* **51**, 212 (1995).
- [20] F. F. Karney, A. B. Rechester, and R. B. White, *Physica D* **4**, 425 (1982).
- [21] G. Taylor, *Proc. R. Soc. London, Ser. A* **219**, 186 (1953).
- [22] We have verified our main results using different area-preserving maps and coupling potentials.
- [23] In order to avoid artificial symmetries we choose  $K_i \in [0.51, 0.53]$ ,  $i \in \{2..N\}$  and fix  $K_1 = 0.52$ . We use the projection into  $(q_1, p_1)$  to facilitate the comparison with the RTS of the noisy system, but similar results are obtained in the full phase space.
- [24] Inside the island  $q_i \in [0.45, 0.55]$ ,  $p_i \in [0.4, 0.6]$  for  $i \in \{2, \dots, N\}$  and close to it  $q_1 = 0.65$ ,  $p_1 \in [0.835, 0.845]$  in the remaining map.